Title: Easy and inexpensive method for the visual and electronic detection of oxidants in air by using vinylic films with embedded aniline

Authors: Blanca S. Pascual, Saúl Vallejos, José A. Reglero Ruiz, Juan C. Bertolín, César Represa, Félix C. García, José M. García

PII: S0304-3894(18)30948-8
DOI: https://doi.org/10.1016/j.jhazmat.2018.10.039
Reference: HAZMAT 19860

To appear in: *Journal of Hazardous Materials*

Received date: 12-4-2018
Revised date: 12-10-2018
Accepted date: 13-10-2018

Please cite this article as: Blanca S.Pascual, Saúl Vallejos, José A.Reglero Ruiz, Juan C.Bertolín, César Represa, Félix C.García, José M.García, Easy and inexpensive method for the visual and electronic detection of oxidants in air by using vinylic films with embedded aniline, Journal of Hazardous Materials https://doi.org/10.1016/j.jhazmat.2018.10.039

Easy and inexpensive method for the visual and electronic detection of oxidants in air by using vinylic films with embedded aniline

Blanca S. Pascual,[ł] Saúl Vallejos,[ł] José A. Reglero Ruiz,[ł,*] Juan C. Bertolín,[ǂ] César Represa,[ǂ] Félix C. García,[ł] José M. García.[ł]

[ł] Departamento de Química, Facultad de Ciencias, Universidad de Burgos, Plaza de Misael Bañuelos, s/n, 09001, Burgos, Spain.

[ǂ] Departamento de Ingeniería Electromecánica. Área de Tecnología Electrónica. Escuela Politécnica Superior, Universidad de Burgos, Avda. Cantabria, s/n, 09006, Burgos, Spain.

* Corresponding author: jareglero@ubu.es. Tel: +34 947 258 085; Fax: +34 947 258 831.

Graphical abstract

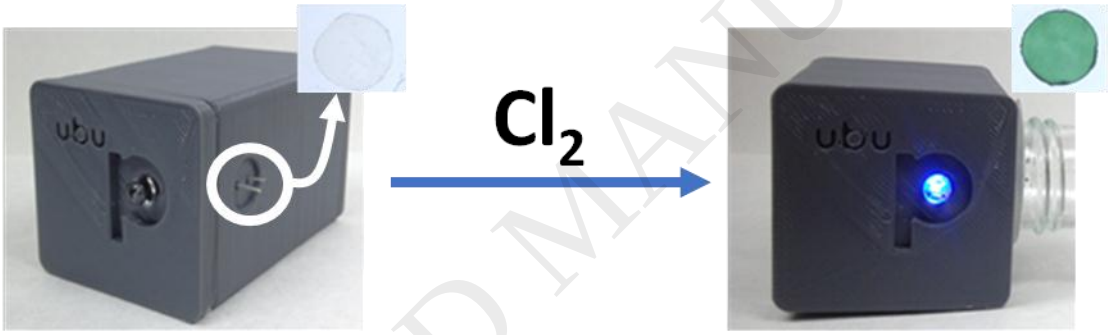

Highlights

- Sensory polymeric materials change their colour in presence of oxidant atmospheres.
- The sensory materials are films shaped with embedded aniline.
- The detection and quantification are based both on optical and electrical methods.
- The detection is achieved visually and also using conventional and simple devices.
- The presence of oxidants Cl_2 and H_2O_2 in air is detected in the ppb_v range.

Abstract

Conventional nonconductive vinylic films with dispersed aniline change their color and become conductive in the presence of specific oxidant gases, namely, chlorine and hydrogen peroxide.

The color change arises from the polymerization of the aniline to yield the conjugated polymer polyaniline, which at the same time renders the flexible vinylic films conductive. We present a simple and straightforward method using both colorimetric and electrical responses to detect and quantify the presence of oxidants (Cl_2 and H_2O_2) in the air. Using RGB analysis (red, green and blue parameters defining the colors in digital pictures on a computer display) based on different pictures taken with a smartphone of discs extracted from the films and by measuring the UV-vis spectral variation in the presence of different concentrations of Cl_2 and H_2O_2, we obtained limits of detection and quantification between 15 and 200 ppb_v for H_2O_2 and between 37 and 583 ppb_v for Cl_2. Additionally, the electrical response was measured using a fabricated device to visually detect the electrical conductivity activation of the sensor in the presence of oxidant atmospheres, detecting a rapid decrease in resistivity (three orders of magnitude) when the polymerization of aniline began, changing the film from non-conductive to conductive.

Keywords: vinylic films; detection of oxidant atmospheres; visual detection; resistivity sensors; conductive polymers

1. Introduction

We present herein the straightforward and inexpensive detection of oxidant agents, such as hydrogen peroxide (H_2O_2) and chlorine (Cl_2), in air. The detection of these compounds is useful from a civil security and military point of view; chlorine has been used as a chemical warfare agent (CWA) since World War I [1], and hydrogen peroxide has been used to prepare homemade explosives, such as triacetone triperoxide (TATP), recently used in terrorist attacks in Europe [2].

Many authors have described the detection of these oxidants by exploiting polymers, including polyaniline (PANI), as piezoelectric, chemomechanical, electrochemical, colorimetric and fluorescence sensors [3-4,5,6,7,8,9,10,11]. Regarding PANI, numerous works are found in the literature employing nanocomposite materials based on PANI to detect different oxidant atmospheres. PANI-MnO_2 nanofibers were used to electrochemically determine [H_2O_2], with limit of detection (LOD) values of 0.1 mM [12]. Core-shell polycaprolactone-PANI fibers were

employed to detect ammonia gas, with a LOD of 1 ppm [13]. Additionally, silver-PANI nanocomposites (such as nanorods) were used to detect [H_2O_2] with LODs of 0.13 to 1.12 µM [14]. Different PANI nanoparticles with reduced graphene oxide (RGO) have been used as sensors for ammonia, with a LOD of approximately 50 ppm [15]. In addition, the review presented by Fratoddi *et al.* describes the use of different nanofibers based on PANI as chemoresistance sensors to detect different gases with a LOD of 20 ppm [16]. PANI has also been used in thin films to detect alcohol vapors using quartz crystal microbalances [17] and in titanium (IV) phosphate nanocomposites to detect ammonia vapors [18]. Other recent works presented by several authors have analyzed the detection of humidity using organic/inorganic polyaniline-based nanocomposites [19,20], the quantification of 4-nitrophenol using Ag nanowire/PANI nanocomposites with a LOD of 0.6 µM [21], and biological applications, such as the immobilization of alpha-fetoprotein by electrochemical biosensing using microporous PANI, with a LOD of 3.7 fg·mL^{-1} [22]. All these works dealt with sensory materials and nanomaterials using previously prepared, purified and isolated PANI.

Additionally, different works have analyzed the polymerization of aniline in the presence of oxidant atmospheres, as in the classical work of Sun *et al.* [23] or the recent work of Sapurina *et al.* [24] However, the novelty of our research lies not specifically in the chemical polymerization of aniline, but in the use of vinylic films in which the aniline can be easily embedded and in the subsequent employment of these films as cheap and straightforward sensory materials to detect and quantify the presence of different oxidant atmospheres in the air. It is known that different pollutants can be tested in this detection process (SO_2, O_2, F_2, Br_2, I_2, H_2O_2, Cl_2 or O_3). However, we focused our analysis on two different oxidants (Cl_2 and H_2O_2) that are reported to effectively produce the oxidation of aniline and the formation of the conductive form of PANI. [**Error! Bookmark not defined.**,25] Then, we proposed the dispersion of aniline within a colorless, flexible and electrically isolating vinylic film that turns the material into a highly colored and conductive film comprised of a vinylic matrix containing PANI sequences. Color change was detected visually and quantified using pictures taken with a smartphone, following a

similar procedure to that exposed in other previous works, in which the luminescence variation in digital pictures of different paper sensors for pesticides was analyzed by means of RGB determination using a smartphone [26], or for example the RGB analysis of different contaminants in food-safety inspection [27]. We also included the analysis of color variation using a UV-vis spectrometer. Finally, we employed a third detection technique based on the electrical resistivity variation, which can indicate within seconds the presence of oxidants (through an electrical output measured in situ and by means of a visual signal by closing an electrical circuit that turns on an LED when aniline becomes conductive due to the oxidation). Compared to the literature and specially the detection methods based on aniline nanocomposites, our measurement methodology and material preparation are easier and inexpensive, which simplifies the fabrication methods and leads to easy-to-handle films, assuring an optimal dispersion of the aniline in the sensory device and avoiding, for example, the typical agglomeration problems associated with nanocomposite-based materials. Additionally, these films are stable with time and can be used by unskilled personnel to inexpensively detect oxidant atmospheres within seconds at the ppb level. Finally, our work presents a novel mechanism of the detection of oxidants in phase gas, based on the *in situ* solid-state polymerization of aniline, which gives rise, for example, to colorimetric changes that can be detected by the naked eye.

2. Experimental

2.1 Materials

All materials and solvents were commercially available and used as received unless otherwise indicated. The following materials and solvents were used: 1-vinyl-2-pyrrolidone (VP) (Merck, > 98%), methyl methacrylate (MMA) (Aldrich, 99%), 2-hydroxyethyl acrylate (A2HE) (Alfa Aesar, 97%), methacrylic anhydride (AM) (Alfa Aesar, 94%), 2,2-dimethoxy-2-phenylacetophenone (PI) (Aldrich, 99%), sulfuric acid (AnalaR Normapur VWR, 95%), hydrogen peroxide (VWR Prolabo Chemicals, 33%), aniline (Sigma-Aldrich, 99%) distilled under reduced pressure, and commercial bleach (Auchan, sodium hypochlorite < 5%). Aqueous

solutions were prepared using ultrapure water (resistivity of 18.2 MΩ·cm, Milli-Q Direct 8, Millipore).

2.2 Measurements and instrumentation

Pictures of sensory discs (**F1a**) were taken with an iPhone 5S digital camera. The RGB parameters for each disc were obtained directly after taking the pictures with the smartphone using the app called ColorMeter, which automatically averaged the data in a region of 11x11 (121) pixels. A 3D printed light box was used to collect the photos. The homemade 3D-printed (material: polylactic acid) light box (10.7 cm x 17.3 cm x 12.9 cm) used an LED display as the source of light, providing a very constant and reproducible light and obtaining high-quality photos. UV-vis measurements were carried out in a Diode Array Spectrophotometer 8452, Hewlett Packard. The RGB calculation parameter software itself carried out an average determination of the red, green and blue values in a region of the disc; thus, we directly used the values provided by the image analysis software. The experimental error associated with the UV-vis spectrophotometer measurements was approximately 0.1%, corresponding to the precision of the equipment.

The visual alarm system was based on a new 3D-printed light emitting sensory system (material: polylactic acid, dimensions: 6.3 cm x 4 cm x 4 cm), which allowed the detection of the *in situ* formation of the conductive form of PANI, green emeraldine salt (ES), by activating the blue LED incorporated in the system. Finally, the electrical conductivity measurements were carried out using a four-probe sensor (JANDEL®) and an inductive coil integrated in an electronic board (LDC1101 and MPS430) (see description in the Electronic Supplementary Information, ESI, section S1.3).

2.3 Film preparation

The sensory materials were vinylic films [28-29,30] charged with aniline species. The cross-linked films were prepared by photoinitiated bulk radical polymerization in a silanized glass mold (115 µm thick) in an oxygen-free atmosphere. The fabrication procedure and the setup

employed can be found in our previous work [**Error! Bookmark not defined.**]. Our method presents several advantages with respect to other film fabrication procedures, such as bubble electrospinning [31]. For example, we can produce large films (20x20 cm^2) of a controlled thickness (10-200 µm) in a simple polymerization method using a UV lamp or a furnace. To fabricate the films, a solution of the comonomers was prepared, adding the PI last. To assure a homogeneous mixture, the solution was sonicated, helping to release oxygen, which could interfere with the radical PI. The solution was injected in the glass mold and exposed to UV light (250 w UV mercury lamp, Philips HPL-N, emission bands in the UV region at 304, 314, 335, and 366 nm with the maximum emission at 366 nm) for 2 h.

For the preparation of the film **F1**, the following comonomers were employed: VP and MMA in a comonomer ratio of 50% VP and 50% MMA; AM at a mol percentage of 1 with respect to the overall comonomer molar content; and 0.16 wt. % PI as a radical photoinitiator.

Similarly, the preparation of the second film **F2** was carried out using these comonomers: A2HE and MMA in a comonomer ratio of 50% A2HE and 50% MMA; AM at a mol percentage of 1 with respect to the overall comonomer molar content; and 0.16 wt. % of PI as the photoinitiator.

This monomer molar ratio and the addition of the crosslinker assured excellent handleability combined with a good swelling behavior, which is the first in this kind of sensory film.

The films were demolded, washed with running water for one hour, and dried in air. Several samples of both films (100 cm^2) were obtained with good reproducibility, presenting easy handleability.

To achieve the sensory behavior, the films (**F1** and **F2**) were immersed into an aqueous solution of aniline in acidic media (H_2SO_4), to give **F1a** and **F2a**. The charging process required a solution of aniline (20 mmol, 1.82 mL, 0.44 M) in ultrapure water (45 mL) with 95% sulfuric acid (55.62 mmol, 3.12 mL, 1.24 M). This immersion was carried out in a 250-mL beaker. This

process was carried out at room temperature within 2 hours with no stirring. After the charging process, the films were removed from the solution. The remaining drops of the solution were superficially dried with paper. During this process, the films were kept as smooth as possible to make subsequent treatment easier. The films were dried for one hour in air, and afterwards, the surfaces were carefully cleaned with a wet paper to remove the rest of the anilinium salt. Finally, the films were cut into 8 mm discs.

Several preliminary tests were performed for different purposes. First, the optimization of the measurement processes (RGB, representing the red, green and blue colors on a computer display, UV-vis and specially the novel setup to determine the electrical resistivity variation) was conducted. Second, we selected the comonomers, proportions and charging conditions to obtain optimized films in terms of wettability, handleability and flexibility. Finally, we focused our work on two different pollutants (Cl_2 and H_2O_2) that assured the oxidation of the aniline, in order to cause polymerization and obtain the conductive form. Concerning the repeatability of the measurements, we performed two repetitions of each measurement with discs extracted from the same F1a and F2a films, obtaining comparable results.

Figure 1a and 1b present the chemical structure and the photographs of the prepared films. We performed different SEM measurements on the surfaces of the films (see Figure S12 in section S4 of the ESI). All the films presented a flat surface without any specific surface morphology, probably due to the confinement of the films between two silanized glasses during the polymerization process.

Figure 1.

3. Results and discussion

The films showed moderate hydrophilic character (water swelling percentage of 47% for **F1** and 27% for **F2**), which allows the films to be charged with the acidic species of aniline after immersion for 2 h in 45 mL of water containing 1.82 mL of aniline and 1.56

mL of sulfuric acid, thus transforming the films into the oxidant-sensory materials (**F1a** and **F2a**, respectively). The swelling behavior was determined following a simple previously described procedure [**Error! Bookmark not defined.**].

The measurements of **F1a** with the 4-probe sensor were not reproducible because of the bad contact between the film and the metallic tips. **F2a** was synthesized to overcome this problem, as **F2a** was more flexible than **F1a** and the tips could slightly penetrate the film, assuring good electrical contact. Then, **F1a** was used in all the experiments in which colorimetric and UV-vis detection and LED sensors were employed, and **F2a** was employed in the detection process with the four-point probe/inductive sensor, due to its flexibility.

3.1 RGB analysis

F1a responded to oxidant substances in the gaseous and vapor states by developing a deep color, thus allowing the detection of harmful atmospheres. Oxidant atmospheres containing Cl_2 and H_2O_2 gas were created using different amounts of aqueous solutions of commercial H_2O_2 (33% aq.) and commercial bleach (5% in NaClO aq.) for chlorine. It is important to remark that the gas concentration of Cl_2 and H_2O_2 inside the vial was estimated from the liquid concentration of the prepared solutions through the volume of the vial, obtaining the estimated values listed in Table S1 of the ESI. Then, in the case of H_2O_2, it can be easily assumed that all of the initial liquid pollutant concentration transformed to the gas phase. For the Cl_2 atmosphere, the drying of the bleach inside the vials renders principally NaClO at different hydration levels, which decomposes mainly to Cl_2 and O_2, catalyzed by the carbon dioxide present in the air, and probably also to other species. Thus, in this study, the concentration of Cl_2 in the vials used for the tests was calculated assuming that all the NaClO decomposes to Cl_2, and for the abovementioned reason, this value is an approximation. Detailed information on the preparation of the oxidant atmospheres can be found in the ESI, Section S1.1. We performed the preliminary interference tests using CO_2, O_2, N_2, O_3, SO_2 and NO_x gases, observing that the detection

results of H_2O_2 and Cl_2 were not affected by the presence of these gases (see Table S4 in section S5 of the ESI, showing the color developed by the discs in the presence of different oxidants).

The color developed by the colorless **F1a** depends on the oxidant. Both oxidants, Cl_2 and H_2O_2, induced the polymerization of aniline to give PANI; in the case of hydrogen peroxide, the resulting PANI was brown due to the formation of electrically isolating oligomers. On the other hand, with chlorine, the PANI formed corresponds to the green conductive emeraldine salt as it can be seen clearly in the color evolution of the discs presented in Figure 2a and 2b. To determine the presence of the PANI, we performed some preliminary FTIR experiments in the films before and after the sensing process under a Cl_2 atmosphere, finding a peak variation at approximately 3000 cm^{-1} in the films with PANI, thus evidencing the presence of conductive emeraldine salt due to the induced polymerization process [32] (see section S3 in the ESI).

Figure 2.

The color development in **F1a** was used to quantify the concentration of the oxidant in air by using two different techniques: a) RGB parameters, based on processing a picture taken with a smartphone or digital camera in a retroilluminated homemade light box (see ESI for details, section S1) and b) UV-vis spectroscopy. The analysis of the photographs taken of the sensory materials is a simple, inexpensive, and efficient way of measuring concentrations. We employed a commercial software to extract the RGB color model, following the procedure described in section 2.2. Afterwards, the RGB parameters can combined into one variable (PC1, principal component 1) by the principal analysis (PCA) procedure [33,34], allowing for the construction of simple titration curves where a relationship between PC1 and oxidant concentration can be observed (see Figures 3a and 3b). To obtain a direct relation between PC1 and the oxidant concentration, we did not use

the highest values of Cl_2 and H_2O_2 concentrations and employed only the data below 157 ppb and 347 ppb for Cl_2 and H_2O_2, respectively, as described in the caption of Figure 3. Details of the PCA analysis can be found in Tables S2 and S3 in the ESI.

Figure 3.

3.2 UV-vis analysis

The analysis of the sensory discs of **F1a** upon exposure to oxidant atmospheres by UV-vis is shown in Figures 4a, 4b, 4c and 4d, from which titration curves are built. Limits of detection in the ppb_v range were obtained from the titration curves built with RGB and UV-vis data, as depicted in Table 1. Compared to the UV-vis results, which require a long data treatment time and the use of specific equipment, the simple and straightforward use of pictures taken of the **F1a** sensory discs is a costless and instant way of implementing an analytical technique based on everyday technology, e.g., smartphones. However, UV-vis analysis provides a better dynamic range.

Figure 4.

Table 1.

3.3 Electrical conductivity measurements

In the case of detection of chlorine, in addition to the change in color, the polymerization of the aniline dispersed in the films leads to the green electrically conductive form of PANI, called emeraldine salt (ES). Accordingly, the detection of Cl_2 can be carried out by measuring the resistivity of the vinylic films during the formation of the ES. Then, two different detection devices were developed.

First, a visual alarm system consisting of an open electrical circuit with an LED light was developed. This circuit can be closed with a conductive material, switching on the light. This system provides a qualitative detection of chlorine in air (see ESI, Figure S6), working as a visual alarm. Figures 5a, 5b and 5c present the visual system, which can also be designed as a sound alarm.

Figure 5.

Second, a four-point probe/inductive sensor was used to quantitatively measure the electrical behavior of the sensory film **F2a** during the process of detection, showing a decrease in resistivity due to the formation of the conductive ES (see ESI, Figures S7 to S10 in Section S1.3, for details).

Combining the data from the four-point probe sensor and the inductive sensor, it is possible to observe the evolution of resistivity, measured in Ohms per square, of the sensory film **F2a** in the presence of chlorine (Figure 6). The resistivity of the film decreases due to the formation of the conductive form of PANI, emeraldine salt (ES). Moreover, a quick resistivity drop in the material, up to three orders of magnitude, was observed within the first half-minute of measurement, thus pointing to the applicability of the system in the rapid detection of harmful atmospheres.

Figure 6.

4. Conclusions

Briefly, we have developed the synthesis of simple and inexpensive vinylic films with embedded aniline for the visual and electrical detection of oxidant atmospheres (chlorine and hydrogen peroxide). The presence of oxidants in the environment of the sensory films caused a color change in the films that can be seen by the naked eye and easily quantified by analyzing pictures taken of the films. The color change is accompanied by the development of conductivity,

and this property can be used to indicate the presence of oxidants using a four-point probe/inductive sensor or even an extremely simple electrical circuit with an LED light, then developing a visual alarm device in which the light turns on in the presence of oxidants. The vinylic-based films are easily prepared, and after the charging process with aniline, the films can be stored under normal conditions for several weeks before the sensing process, thus presenting an excellent shelf life. The sensory films are truly dosimeters because the sensing comes from the irreversible polymerization of the aniline, so the films cannot be reused.

Funding

The financial support provided by FEDER (Fondo Europeo de Desarrollo Regional) and the Spanish Agencia Estatal de Investigación (AEI) (MAT2017-84501-R) is gratefully acknowledged.

References

1. E. Croddy, C. P. Armendariz, J. Hart. Chemical and Biological Warfare. New York: Springer-Verlag, 2002.

2. M. Burks, D. S. Hage, Current trends in the detection of peroxide-based explosives, Anal. Bioanal. Chem. 395 (2009) 301-313.
3. J. M. García, J. L. Pablos, F. C. García, F. Serna, Sensory Polymers for Detecting Explosives and Chemical Warfare Agents, in Industrial Applications for Intelligent Polymers and Coatings, Springer-Verlag, 2016.
4. J. M. García, F. C. García, F. Serna, J. L. de la Peña, Fluorogenic and chromogenic polymer chemosensors, Polym. Rev. 51 (2011) 341-390.
5. J. P. Lock, E. Geraghty, L.C. Kagumba, K. K. Mahmud, Trace detection of peroxides using a microcantilever detector, Thin Solid Film 517 (2009) 3584-3587. DOI: 10.1016/j.tsf.2009.01.062.

6. A. Mills, P. Grosshans, E. Snadden, Hydrogen peroxide vapour indicator, Sens. Actuators B 136 (2009) 458-463.
7. J. C. Sánchez, W. C. Trogler, Polymerization of a boronate-functionalized fluorophore by double transesterification: applications to fluorescence detection of hydrogen peroxide vapor, J. Mater. Chem. 18 (2008) 5134-5141.
8. Y. Fang, D. Zhang, X. Qin, Z. Miao, S. Takahashi, J-I. Anzai, Q. Chen, A non-enzymatic hydrogen peroxide sensor based on poly(vinyl alcohol)-multiwalled carbon nanotubes-platinum nanoparticles hybrids modified glassy carbon electrode, Electrochim. Acta, 70 (2012) 266-271.
9. J. Tian, H. Li, W. Lu, Y. Luo, L. Wanga, X. Sun, Preparation of Ag nanoparticle-decorated poly(m-phenylenediamine) microparticles and their application for hydrogen peroxide detection, Analyst 136 (2011) 1806-1809.
10. Z. Wu, S. Yang, Z. Chen, T. Zhang, T. Guo, Z. Wang, F. Liao, Synthesis of Ag nanoparticles-decorated poly(m-phenylenediamine) hollow spheres and the application for hydrogen peroxide detection, Electrochim. Acta 98 (2009) 104-108.
11. C. Li, J. Hu, T. Liu, S. Liu, Stimuli-triggered off/on switchable complexation between a novel type of charge-generation polymer (CGP) and gold nanoparticles for the sensitive colorimetric detection of hydrogen peroxide and glucose, Macromolecules 44 (2011) 429-431.
12. J-H. Lee, H-G. Hong, Nonenzymatic electrochemical sensing of hydrogen peroxide based on a polyaniline-MnO2 nanofiber-modified glassy carbon electrode, J. Appl. Electrochem. 45 (2015) 1153-1162.
13. W. Zhou, Y. Guo, H. Zhang, y. Su, M. Liu, B. Dong, A highly sensitive ammonia sensor based on spinous core–shell PCL–PANI fibers, J. Mater. Sci. 52 (2017) 6554-6566.
14. F. Lorestani, P. Moozarm Ni, Y. Alias, N. S. A. Manan, One-step synthesis of different silver-polyaniline composite morphologies for enzymeless hydrogen peroxide detection, J. Electrochem. Soc. 162 (2015) B193-B200.

15. X. Huang, N. Hu, R. Gao, Y. Yu, Y. Wang, Z. Yang, E. Siu- Wai Kong, H. Wei, Y. Zhang, Reduced graphene oxide–polyaniline hybrid: Preparation, characterization and its applications for ammonia gas sensing, J. Matter. Chem. 22 (2012) 22488-22495.
16. I. Fratoddi, I. Venditti, C. Cametti, M. V. Russo, Chemiresistive polyaniline-based gas sensors: A mini review, Sens. Actuators B 220 (2015) 534-548.
17. M. M. Ayad, G. El-Hefnawey, N. L. Torad, A sensor of alcohol vapours based on thin polyaniline base film and quartz crystal microbalance, J. Hazard. Mater. 168 (2009) 85-88.
18. A. A. Khan, U. Baig, M. Khalid, Ammonia vapor sensing properties of polyaniline-titanium(IV)phosphate cation exchange nanocomposite, J. Hazard. Mater. 186 (2011) 2037-2042.
19. Q. Chen, M. Nie, Y. Guo, Controlled synthesis and humidity sensing properties of CdS/polyaniline composite based on CdAl layered double hydroxide, Sens. Actuators B 254 (2018) 30-35.
20. D. Zhang, D. Wang, P. Li, X. Zhou, X. Zong, G. Dong, Facile fabrication of high-performance QCM humidity sensor based on layer-by-layer self-assembled polyaniline/graphene oxide nanocomposite film, Sens. Actuators B 255 (2018) 1869-1877.
21. C. Zhang, S. Govindaraju, K. Giribabu, Y. S. Huh, K. Yun, AgNWs-PANI nanocomposite based electrochemical sensor for detection of 4-nitrophenol, Sens. Actuators B 252 (2017) 616-623.
22. S. Liu, Y. Ma, M. Cui, X. Luo, Enhanced electrochemical biosensing of alpha-fetoprotein based on three-dimensional macroporous conducting polymer polyaniline, Sens. Actuators B 255 (2018) 2568-2574.
23. Z.C. Sun, Y.H. Geng, J. Li, X.B. Jing, F.S. Wang, Chemical polymerization of aniline with hydrogen peroxide as oxidant, Synthetic Met. 84 (1997) 99-100.
24. I.Y. Sapurina, J. Stejskal, Oxidation of aniline with strong and weak oxidants, Russ. J. Gen. Chem. 82 (2012) 256-275.

25. X. Li, X. Li, Oxidative polymerization of aniline using $NaClO_2$ as an oxidant, Mater. Lett. 61 (2007) 2011-2014.
26. Q. Mei, H. Jing, Y. Li, W. Yisibashaer, J. Chen, B.N. Li, Y. Chang, Smartphone based visual and quantitative assays on upconversional paper sensor, Biosens. Bioelectron. 75 (2016) 427-432.
27. Z. Liu, Y. Zhang, S. Xu, H. Zhang, Y. Tan, C. Ma, R. Song, L. Jiang, C. Yi, A 3D printed smartphone optosensing platform for point-of-need food safety inspection, Anal. Chim. Acta 966 (2017) 81-89.
28. S. Vallejos, A. Muñoz, S. Ibeas, F. Serna, F. C. García, J. M. García, Forced solid-state interactions for the selective "turn-on" fluorescence sensing of aluminum ions in water using a sensory polymer substrate, ACS Appl. Mater. Interfaces 7 (2015) 921-928.
29. S. Vallejos, A. Muñoz, F. C. García, R. Colleoni, R. Biesuz, G. Alberti, J. M. García, Colorimetric detection, quantification and extraction of Fe(III) in water by acrylic polymers with pendant Kojic acid motifs, Sens. Actuators B 233 (2016) 120-126.
30. S. Vallejos, J. A. Reglero, F. C. García, J. M. García, Direct visual detection and quantification of mercury in fresh fish meat using facilely prepared polymeric sensory labels, J. Mater. Chem. A 5 (2017) 13710-13716.
31. H. Dou, H. Liu, P. Wang, J-H. He. A belt-like superfine film fabricated by the bubble-electrospinning, Therm. Sci. 17 (2013) 1508-1510.
32. J. Stejskal, M. Trchová, Aniline oligomers versus polyaniline, Polymer 61 (2011) 240-251.
33. G. Foca, F. Masino, A. Antonelli, A. Ulrici, Prediction of compositional and sensory characteristics using RGB digital images and multivariate calibration techniques, Anal. Chim. Acta 706 (2011) 238-245.
34. S. Vallejos, A. Muñoz, S. Ibeas, F. Serna, F. C. García, J. M. García, Solid sensory polymer substrates for the quantification of iron in blood, wine and water by a scalable RGB technique, J. Mater. Chem. A 1 (2013) 15435-15441.

Caption of Figures

Figure 1. Scheme of the chemical composition of: a) **F1** and b) **F2** with Photographs of the films (**F1** and **F2**) and sensory films (**F1a** and **F2a**).

Figure 2. Sensory response of F1a discs to: a) Chlorine, [Cl_2]: blank, 16, 39, 79, 118, 157, 394, 787, 1180 and 1574 ppb_v; b) Hydrogen peroxide, [H_2O_2]: blank, 34, 87, 174, 261, 347, 868, 1737, 2605 and 3474 ppb_v.

Figure 3. Titration curves of F1a discs exposed to oxidants in air: a) Chlorine, [Cl_2] = blank, 16, 39, 79, 118 and 157 ppb_v; b) Hydrogen peroxide, [H_2O_2] = blank, 35, 87, 174, 261 and 347 ppb_v, using RGB parameters, reduced to one principal component (PC1) by principal component analysis. Inset: Relation between PC1 and oxidant concentration at high values.

Figure 4. UV-Vis spectra of **F1a** discs after exposing them to increasing concentration of Cl_2 (a) and H_2O_2 (b) in air; c) Titration curve for chlorine, [Cl_2]: 79, 118, 157, 394, 787, 1180 and 1574 ppb_v; d) Titration curve for hydrogen peroxide, [H_2O_2]: 0, 35, 87, 174, 261, 868 and 1737 ppb_v.

Figure 5. Visual alarm system: a) physical appearance; b) setting of the sensory F1a disc in the metallic terminals; c) blue led switched-on due to the formation of emeraldine salt by the presence of chlorine in the environment of the sensory disc (1 ppm_v).

Figure 6. Evolution of the resistivity of the sensory film **F2a** exposed to chlorine in air, [Cl_2]: 230 ppm_v. [ρ] = Ω/sqr, units of sheet resistance; inset: resistivity drop during the initial 25 s of measurement.

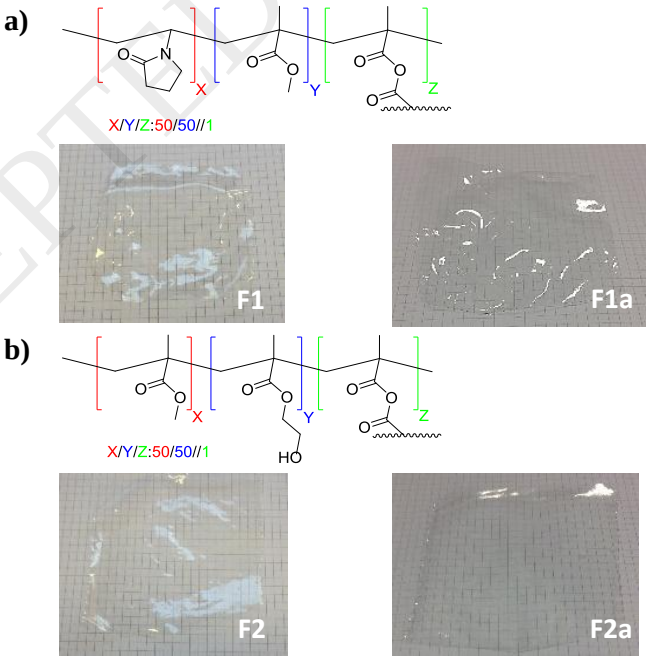

Figure 1. Scheme of the chemical composition of: a) **F1** and b) **F2** with Photographs of the films (**F1** and **F2**) and sensory films (**F1a** and **F2a**).

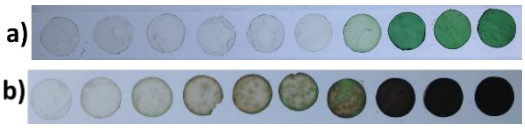

Figure 2. Sensory response of **F1a** discs to: a) Chlorine, [Cl_2]: blank, 16, 39, 79, 118, 157, 394, 787, 1180 and 1574 ppb_v; b) Hydrogen peroxide, [H_2O_2]: blank, 34, 87, 174, 261, 347, 868, 1737, 2605 and 3474 ppb_v.

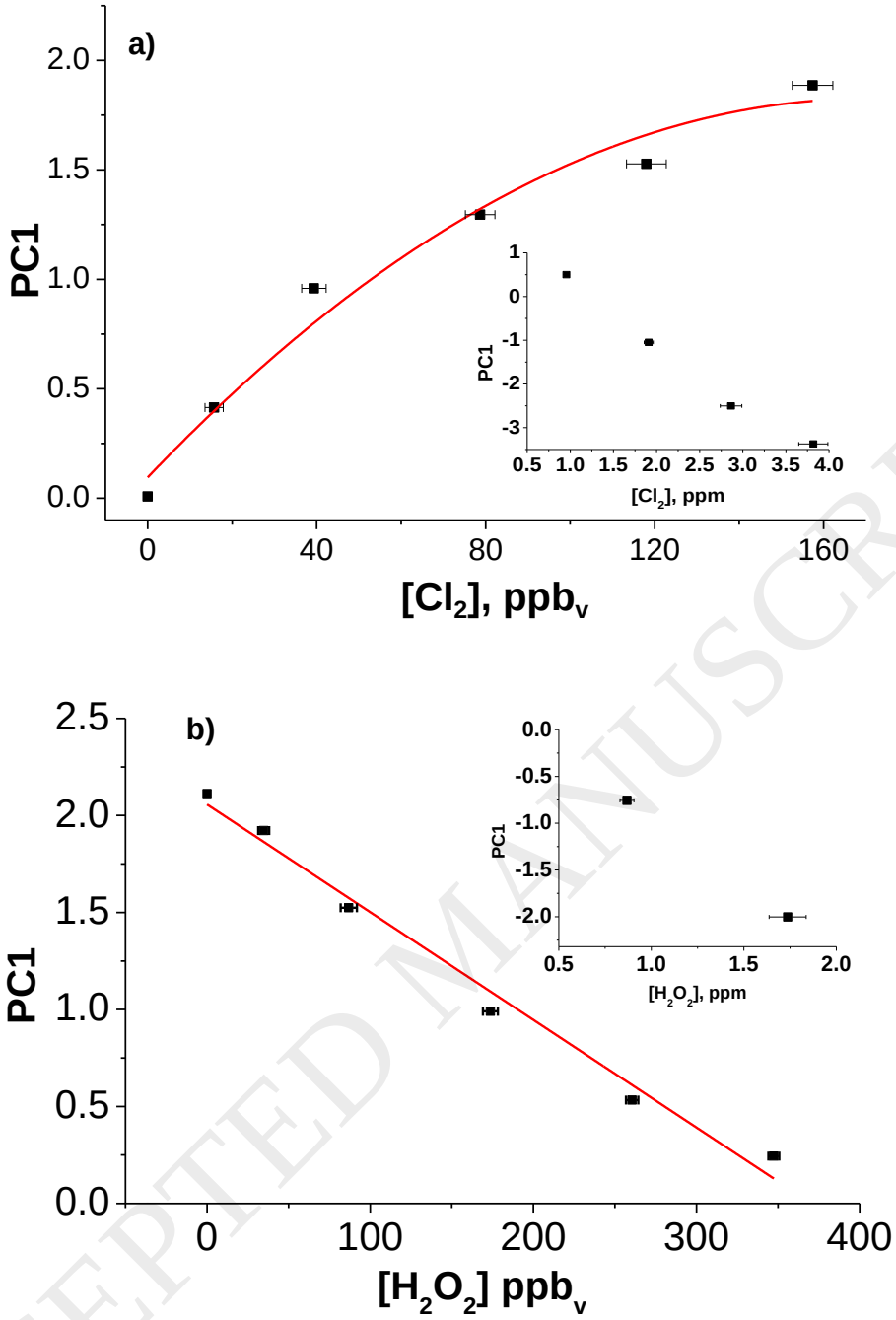

Figure 3. Titration curves of F1a discs exposed to oxidants in air: a) Chlorine, [Cl_2] = blank, 16, 39, 79, 118 and 157 ppb_v; b) Hydrogen peroxide, [H_2O_2] = blank, 35, 87, 174, 261 and 347 ppb_v, using RGB parameters, reduced to one principal component (PC1) by principal component analysis; Inset: Relation between PC1 and oxidant concentration at high values.

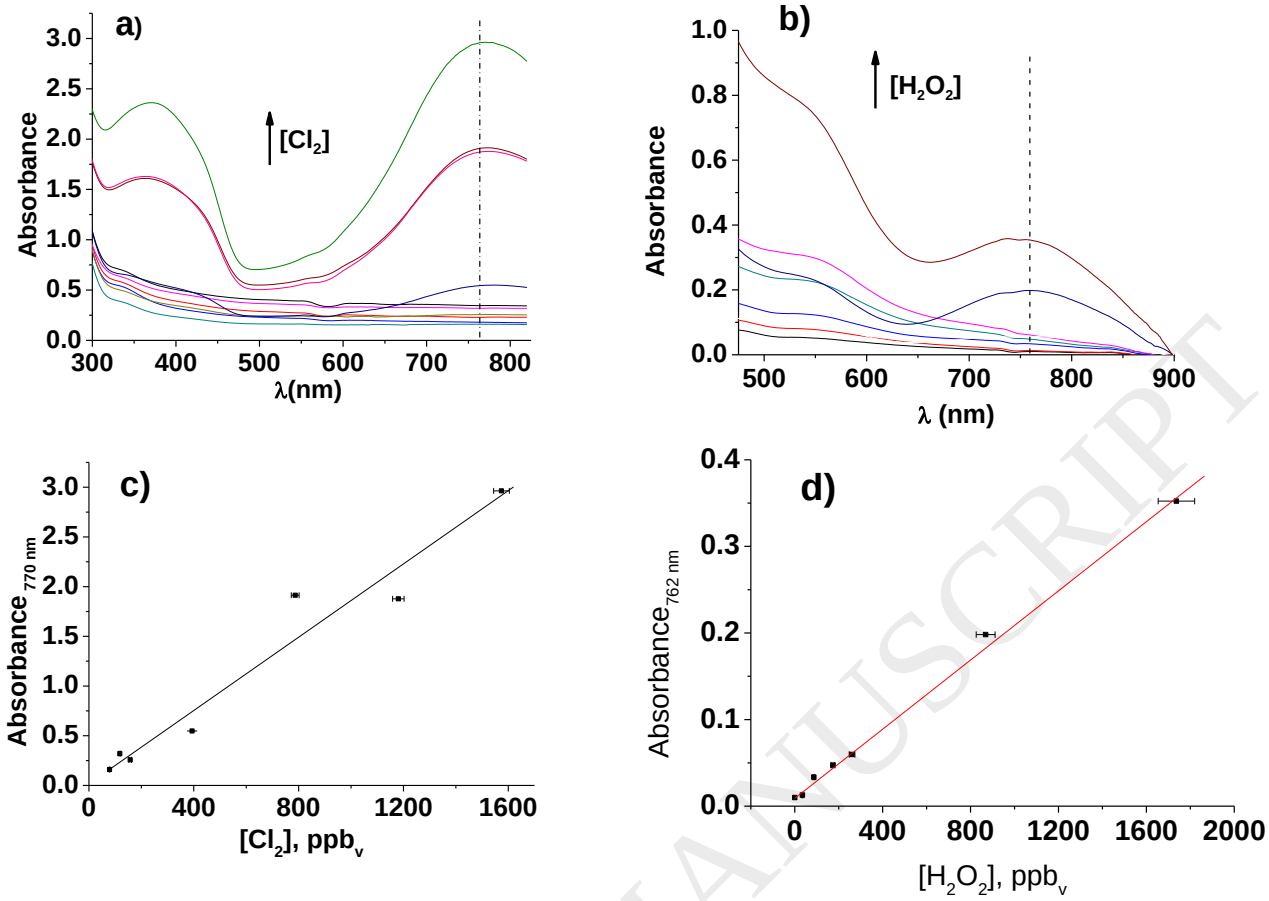

Figure 4. UV-Vis spectra of **F1a** discs after exposing them to increasing concentration of Cl_2 (a) and H_2O_2 (b) in air; c) Titration curve for chlorine, [Cl_2]: 79, 118, 157, 394, 787, 1180 and 1574 ppb_v; d) Titration curve for hydrogen peroxide, [H_2O_2]: 0, 35, 87, 174, 261, 868 and 1737 ppb_v.

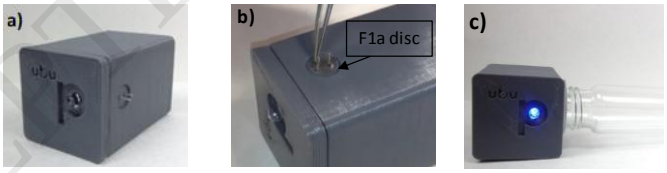

Figure 5. Visual alarm system: a) physical appearance; b) setting of the sensory **F1a** disc in the metallic terminals; c) blue led switched-on due to the formation of emeraldine salt by the presence of chlorine in the environment of the sensory disc (1 ppm_v).

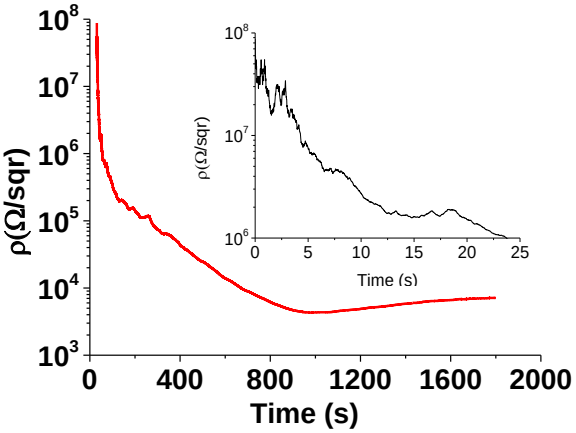

Figure 6. Evolution of the resistivity of the sensory film **F2a** exposed to chlorine in air, [Cl_2]: 230 ppm_v. [ρ] = Ω/sqr, units of sheet resistance; Inset: resistivity drop during the initial 25 s of measurement.